Contact mechanics for soft robotic fingers: modeling and experimentation

Sadeq H. Bakhy†, Shaker S. Hassan†, Somer M. Nacy‡*,
K. Dermitzakis§ and Alejandro Hernandez Arieta§

†Department of Machines and Equipments Engineering, University of Technology, Baghdad, Iraq
‡Department of Manufacturing Operations Engineering, Al-Khwarizmi College of Engineering, Baghdad, Iraq
§Artificial Intelligence Laboratory, Department of Informatics, University of Zurich, Zurich, Switzerland

SUMMARY
Human fingers possess mechanical characteristics, which enable them to manipulate objects. In robotics, the study of soft fingertip materials for manipulation has been going on for a while; however, almost all previous researches have been carried on hemispherical shapes whereas this study concentrates on the use of hemicylindrical shapes. These shapes were found to be more resistant to elastic deformations for the same materials. The purpose of this work is to generate a modified nonlinear contact-mechanics theory for modeling soft fingertips, which is proposed as a power-law equation. The contact area of a hemicylindrical soft fingertip is proportional to the normal force raised to the power of γ_{cy}, which ranges from 0 to 1/2. Subsuming the Timoshenko and Goodier (S. P. Timoshenko and J. N. Goodier, *Theory of Elasticity*, 3rd ed. (McGraw-Hill, New York, 1970) pp. 414–420) linear contact theory for cylinders confirms the proposed power equation. We applied a weighted least-squares curve fitting to analyze the experimental data for different types of silicone (RTV 23, RTV 1701, and RTV 240). Our experimental results supported the proposed theoretical prediction. Results for human fingers and hemispherical soft fingers were also compared.

KEYWORDS: Grasping; Robotic hands; Novel applications of robotics; Humanoid robots; Biomimetic robots.

Notations:

Following are the terms used frequently throughout this work:

Symbols	Definition	Units
a_{cy}	Half width contact of rectangular contact area for hemicylindrical fingertips	mm
a_{sph}	Radius of circular contact area for hemispherical fingertips	mm
b	Half depth contact of rectangular contact area	mm

* Corresponding author. E-mail: somernacy@gmail.com

c_{cy}	Constant that depends on the size, depth, and curvature of the hemicylindrical fingertip	–
d	Displacement of fingertip at the contact zone at $x = 0$	mm
N	Normal force	N
n	Stress exponent for nonlinear elastic materials (strain-hardening factor)	–
$u(x)$	Displacement in the contact zone due to normal force at contact	mm
x, y	Citizen coordinates	–
γ_{cy}	Exponent of the power-law equation for soft hemicylindrical fingertips contacts	–
γ_{sph}	Exponent of the power-law equation for soft hemispherical fingertips contacts	–
σ_e	Von-Mises stress	MPa
$\sigma_{ij}, \epsilon_{ij}$	Stress and strain components in i and j directions	MPa
σ_x, σ_y	Stresses in the x and y axes respectively.	MPa
$\tilde{x}, \tilde{z}$	Nondimensionalized coordinates $\tilde{x} = \frac{x}{a_{cy}}, \ \tilde{z} = \frac{z}{a_{cy}}$.	–
$\tilde{u}_i$	Nondimensionalized displacement in ith direction	–
$\tilde{\sigma}_{ij}, \tilde{\epsilon}_{ij}$	Nondimensionalized stress and stain components	–

1. Introduction
Soft fingers are commonly used as fingertips to provide the means of interaction between prosthetic robotic hands and the environment with which they interact. One of most important mechanical characteristics of fingertips is softness, considered as one of the major differences between robotic fingertips and human fingertips. When manipulating an object, softness plays a big role in the change of contact area between the fingertip and the object. The soft-finger contact model provides more realistic results in robotic grasping and manipulation; the estimation of grasping forces requires knowledge of stiffness and contact characteristics, including

the relationship between normal force and contact area of the fingertip. These factors are considered as a key to dexterous manipulation.[1]

More than a century ago, Hertz[2] studied the growth of contact area as a function of the applied normal force N based on a linear elastic model. He conducted experiments using a spherical glass lens against a planar glass plate. His results showed how the radius of contact was proportional to the normal force raised to the power of 1/3, which was consistent with the analytical results based on the linear elastic model. Timoshenko and Goodier[3] studied the contact between two parallel cylinders. Their results showed analytically the value of contact width of the linear elastic cylinder which was proportional to the normal force raised to the power of 1/2. However, if we visualize an ideal hemicylindrical soft finger, which assumes the entire contact area upon application of the initial normal force, and a further increase in the normal force that does not increase the contact area, then the exponent will be 0 instead of 1/2. Of course, such an ideal soft finger may not exist, but typical soft fingers will behave in-between the two extremes. It is of interest to derive such a model to use the results for optimal grasping and manipulation.

Schallamach[4] and Cutkosky *et al*.[5] explored the performance of various kinds of rubbers in their research for complaint materials that will provide ideal skin for artificial robot fingers. Others have tried to gain insight from the human body as done by Han *et al*.,[6] who designed artificial finger using data obtained from experiments on human subjects. Xydas and Kao[7,8] developed a power-law theory for soft hemispherical fingertips. This power-law theory was suggested for soft fingers, which behaved more like nonlinear contacts. The results showed that the radius of contact (a_{sph}) was proportional to the normal force (N) raised to the power (γ_{sph}), which ranges from 0 to 1/3, i.e.

$$\gamma_{\text{sph}} = \frac{n}{2n+1} \quad 0 \leq n \leq 1. \quad (1)$$

Experiments were conducted to validate the theory using artificial soft fingers made of rubber and silicone. Kao and Yang,[9] based on the power-law theory for hemispherical soft-finger contacts, derived the equation to describe the nonlinear stiffness behavior of soft contacts.

Park *et al*.[10] presented a hemisphere-shaped soft fingertip for soft fingers and modeled a nonlinear force function of a soft fingertip according to the deformation by considering the force distribution in the contact surface. A tactile sensor was used to measure the contact force distribution in the contact surface and its total force. The proposed model was considered for a one-dimensional (1D) finger contact. Inoue and Hirai[11] proposed a straightforward static elastic model of a hemispherical soft fingertip undergoing large contact deformation. They formulated a static elastic force model with an elastic potential energy function based on virtual springs inside a hemispherical soft. The equations are functions of two variables: the maximum displacement of the hemispherical fingertip and the orientation angle of a contacting planar object. The elastic potential energy had a local minimum in the proposed model.

Hosoda *et al*.[12] studied a novel design of an anthropomorphic soft fingertip with distributed receptors. They explored ways to improve the discrimination of materials by pushing and rubbing of objects. The fingertip consisted of two silicone rubber layers of different hardnesses containing two kinds of receptors: strain gauges and polyvinylidene fluoride (PVDF) films. The structure of the fingertip was similar to that of a human fingertip, involving a bone structure, a body, a skin layer, and randomly distributed receptors inside. Experimental results demonstrated the discriminating ability of the fingertip.

Ficuciello[13] adopted a port-Hamiltonian model of a robotic hand with soft pads on fingertips. The viscoelastic behavior of the contact was described in terms of energy storage and dissipation.

Ho and Hirai,[14] constructed a hybrid finite element model to simulate the dynamic behavior of a sliding hemispherical and hemicylindrical soft fingertips. They focused on the stick-slip transition of slide, in which dynamically localized displacements on the contact surface were reproduced. Their experiments gave good validation to the proposed model.

In this paper, we study the nonlinear contact mechanics of hemicylindrical soft fingers through theoretical modeling and experimental validation. We derive a relationship between the normal force and the half width contact area assuming that the materials of anthropomorphic hemicylindrical soft finger with different silicone-based materials (namely, RTV 23, RTV 1701, and RTV 240) are nonlinear elastics. Based on the theory from Hutchinson,[15] we experimentally determine the growth of the contact area with respect to the normal force for typical anthropomorphic hemicylindrical soft fingers. It was found that hemicylindrical shape fingertips are more practical as compared to hemispherical shape, since smaller size hemicylindrical fingertips can afford the same contact properties produced by larger size hemispherical fingertips.

2. Theoretical Approach and Modeling
The main objective of this section is to derive a contact mechanics model, including nonlinear materials, thus representing more realistic soft fingers.

2.1. The linear elastic model: the Timoshenko and Goodier contact model
Hertz[2] provide the first satisfactory analysis of mechanical contact of two elastic solids. He studied the growth of contact area as a function of the applied normal force N, based on the linear elastic model. He conducted experiments using a spherical glass lens against a planar glass plate. The radius of contact is proportional to the normal force raised to the power of 1/3, which is consistent with the analytical results that he derived based on the linear elastic model. Timoshenko and Goodier[3] studied the contact between two parallel cylinders and founded analytically the value of half width contact for a linear elastic cylinder a_{cy}, which is proportional to the normal force N raised to the power of 1/2, i.e.

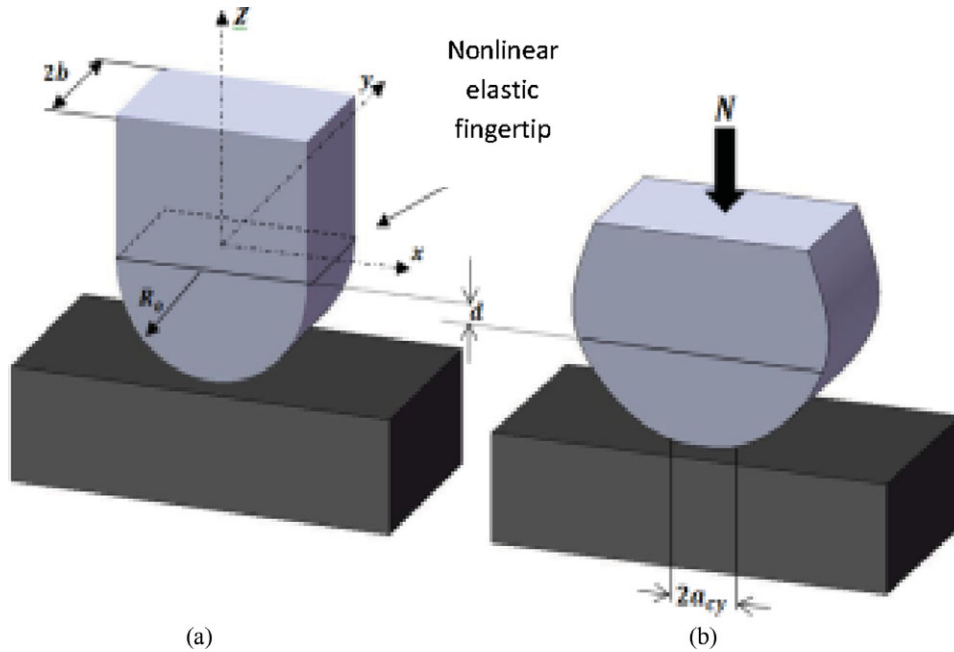$$a_{\text{cy}} \propto N^{\frac{1}{2}}. \quad (2)$$

Fig. 1. (Colour online) (a) Model of a nonlinear elastic cylinder making contact with a surface, pushed by a normal force N (simplified model); and (b) model of a hemicylindrical soft finger being pushed onto a rigid plane. The contact area is assumed to be rectangular.

2.2. The nonlinear elastic model

For incompressible nonlinear elastic materials, the 3D constitutive relation is given by the following equations[7,8,15,16]:

$$\epsilon_{ij} = \left(\frac{\sigma_e}{k_s}\right)^n \frac{\partial \sigma_e}{\partial \sigma_{ij}}, \tag{3}$$

$$\sigma_{ij} = \sigma_e \frac{\partial}{\partial \epsilon_{ij}} \left(\frac{\sigma_e}{k_s}\right)^n; \tag{4}$$

the Von-Mises stress is

$$\sigma_e = \sqrt{\frac{3}{2}\delta_{ij}\delta_{ij}} = \sqrt{\frac{3}{2}\left(\sigma_{ij} - \frac{1}{3}\sigma_{kk}\delta_{ij}\right)\left(\sigma_{ji} - \frac{1}{3}\sigma_{kk}\delta_{ji}\right)}, \tag{5}$$

and the strain components are

$$\epsilon_{ij} = \frac{1}{2}\left(\frac{\partial u_i}{\partial x_j} + \frac{\partial u_j}{\partial x_i}\right) \tag{6}$$

where k_s is a constant with the stress unit, n is a strain hardening factor (i.e. the stress exponent depending on the material ($n \leq 1$)), $\frac{\partial u_i}{\partial x_j}$ is a derivative of u_i with respect to the jth orthogonal coordinate in Cartesian coordinates, and u_i is the infinitesimal displacement. In addition, the stress equilibrium requires that

$$\frac{\partial \sigma_{ij}}{\partial x_j} = 0. \tag{7}$$

Considering a nonlinear elastic cylinder of radius R_o being pushed onto a rigid plane, as shown in Fig. 1, and taking the x and y axes in the direction of the semi-axes a_{cy} and

b respectively, and knowing the boundary conditions at the surface of the rectangular in the Cartesian coordinates, namely

$$\begin{aligned}\sigma_x &= 0 \\ \sigma_y &= 0\end{aligned} \quad \text{for } \begin{aligned}x &> a_{cy} \\ y &> b\end{aligned} \text{(nocontact)}, \tag{8}$$

the displacement in the contact zone due to normal force can be presented as

$$u(x) = d - \left(R_o - \sqrt{R_o^2 - x^2}\right) \quad \text{for } x < a_{cy} \text{ (in contact)}, \tag{9}$$

where b is the half depth of contact, a_{cy} is the half width of contact area, σ_x and σ_y denote the stresses in x and y axes respectively, u is the displacement in the contact zone due to normal force at the contact, and d is the displacement in the contact zone at $x = 0$, as shown in the Fig. 1. Furthermore, the force balance for the contact area requires that

$$N = \int_A \sigma_{zz} dA. \tag{10}$$

In this work, dA is the rectangular contact area of the cylindrical soft finger (assume the depth $2b$ remains constant),

$$N = \int_{-b}^{b}\int_{-a}^{a} \sigma_{zz}\, dx\, dy = 2b \int_{-a}^{a} \sigma_{zz} dx, \tag{11}$$

where σ_{zz} is the stress component normal to the contact surface. Using the following dimensionless variables:

$$\tilde{x} = \frac{x}{a_{cy}}, \tag{12}$$

$$\tilde{u}_i = \frac{u_i R_o}{a_{cy}^2}, \tag{13}$$

$$\tilde{z} = \frac{z}{a_{cy}}, \tag{14}$$

where u_i is given by Eq. (9). Substituting $\tilde{x}$ and $\tilde{u}$ into Eq. (6), we obtain

$$\epsilon_{ij} = \frac{a_{cy}}{R_o} \tilde{\epsilon}_{ij}, \tag{15}$$

where $\tilde{\epsilon}_{ij} = \frac{1}{2}(\frac{\partial \tilde{u}_i}{\partial \tilde{x}_j} + \frac{\partial \tilde{u}_j}{\partial \tilde{x}_i})$. From Eq. (3), after the substitution of ϵ_{ij} in Eq. (15) and σ_e in Eq. (5), one can write,

$$\sigma_{ij} \sim \left(\frac{a_{cy}}{R_o}\right)^{\frac{1}{n}} \tilde{\sigma}_{ij}, \tag{16}$$

where "$\sim$" denotes that σ_{ij} is proportional to $(\frac{a_{cy}}{R_o})^{\frac{1}{n}} \tilde{\sigma}_{ij}$ via dimensional analysis. Substituting Eqs. (12)–(14) and (16) into Eq. (11), yields

$$N = 4b \int_0^{a_{cy}} \sigma_{zz} dr \sim 4b \left(\frac{a_{cy}}{R_o}\right)^{\frac{1}{n}} a_{cy} \int_0^1 \tilde{\sigma}_{zz} d\tilde{r}. \tag{17}$$

The integration of Eq. (17) is dimensionless. By grouping all constant terms, we can write

$$N = c\, a_{cy}^{\frac{1}{n}+1} = c\, a_{cy}^{\frac{1+n}{n}}$$

or

$$a_{cy} = c_{cy} N^{\frac{n}{n+1}} = c_{cy} N^{\gamma_{cy}}, \tag{18}$$

where $\gamma_{cy} = \frac{n}{n+1}$ is the exponent of the normal force, and c_{cy} is a constant that depends on the size and curvature of the fingertip, as well as the material properties. Equation (18) is the new power law that relates the growth of the half width contact with the applied normal force for soft fingers. Note that the equation is derived assuming a rectangular contact area.

For linear elastic materials, the constant n is equal to 1. Thus, Eq. (18) will be the Hertzian contact model for a cylinder:
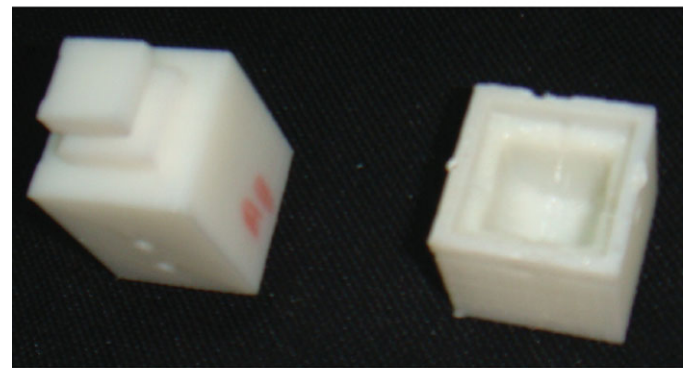
$$a_{cy} = c_{cy} N^{\frac{1}{2}}. \tag{19}$$

Equation (19), a special case of Eq. (18) for linear elastic materials in contact, is in agreement with the Timoshenko and Goodier[3] contact theory. In general, $0 \leq n \leq 1$,[15] therefore the exponent in Eq. (18) is

$$0 \leq \gamma_{cy} \leq \frac{1}{2}. \tag{20}$$

If $\gamma_{cy} = 0$, the width of contact is constant and independent of the normal force. This corresponds to the case of the ideal
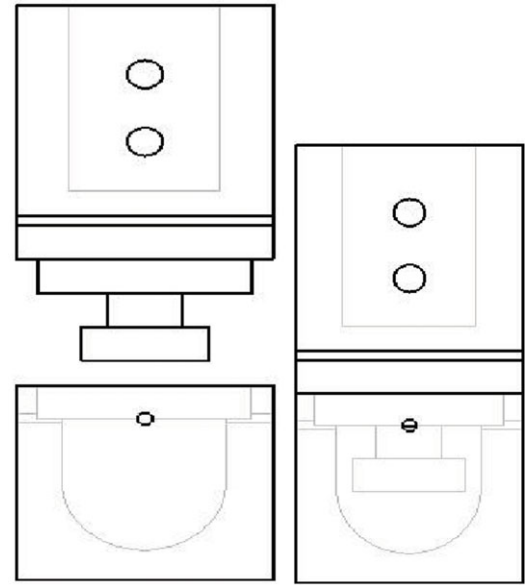
(a)

(b)

Fig. 2. (Colour online) Mold design.

soft finger, where the full contact area is reached once the contact is made, and subsequent increases in the normal force do not increase the area of contact.

3. Experimentations

3.1. Material selection
The soft fingertips were made from three different types of silicone (RTV 23, silicone RTV 1701, and silicone RTV 240), specifically suited for applications similar to do with the present design. Some properties of the silicone used are shown in a Table I.[16]

3.2. Manufacturing of Mold of Robotic Hand Fingertips
Molds for fingertips were prepared and manufactured using rapid prototyping. In this research the mold is designed using Solidwork as shown in the Fig. 2(a), and then manufactured it from ABS solid plastic using a 3D Printer. The mold consists of two parts, shown as an assembled view in Fig. 2(b).

Table I. Silicone materials type for hemicylindrical finger tips with mechanical properties[16].

Silicone type	Hardener	Mixing ratio (%)	Curing time (hours)	Tensile strength (MPa)	Shore A hardness points	Elongation at break (%)	Tear strength (N/mm)	Appearance when cured
RTV 23 (very soft)	A 7	40	24	2.2	6	1000	8	Translucent
RTV 1701(middle)	1701-B	5	8	3.4	17–20	1180	17	White
RTV 240 (hard)	B2	10	24	5.5	40	400	25	Translucent

(a)   (b)
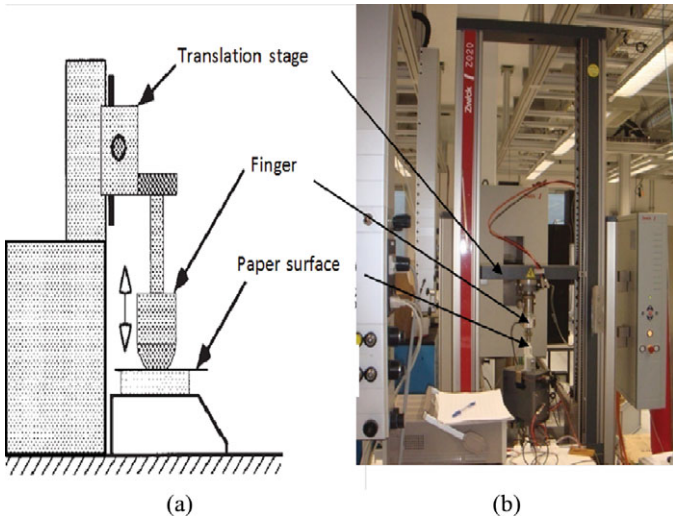
Fig. 3. (Colour online) Experimental set up of the soft-finger contact mechanics model.
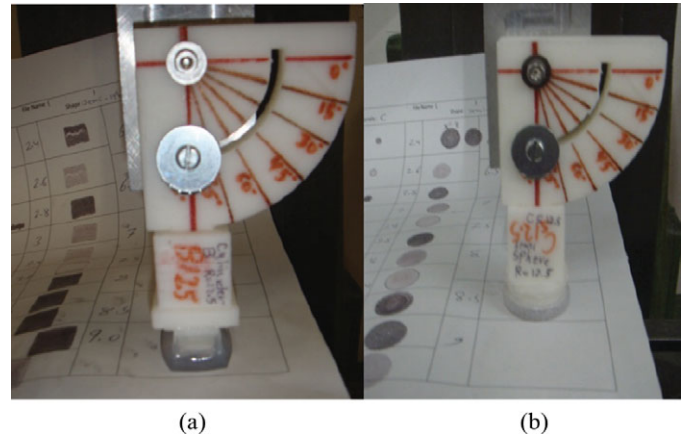

(a)   (b)

Fig. 4. (Colour online) Samples of a finger imprint on recording paper. The finger is coated with fine toner dust, which makes a clear contact imprint on paper surface.

3.3. Experimental validation of contact theory of soft fingertips

The experimental set up used for the verification of the power-law equation (Eq. (18)) is shown in Fig. 3. We used a Zwick tensile tester to measure the force used to press the fingertip on flat solid surface.[17] Each fingertip was fixed on the vertical moving jaw of the machine; when it comes in contact with the flat surface, a normal force is generated and displayed on the readout panel with an accuracy of (± 0.01 N). The area of contact is measured from finger imprints shown in Fig. 4. All the artificial fingers used in the experiments have cylindrical or spherical asperities. The shapes of contact areas are rectangular for the hemicylindrical fingertips as shown in Fig. 4(a), whereas the shapes of contact areas are circular for the hemispherical fingertips as shown in Fig. 4(b). Multiple finger imprints over a range of normal force from $0-100$ N are printed, and the half width and radius contact are measured with accuracy of ± 0.1 mm. All experiments were performed on a smooth surface to avoid possible distortion of finger imprints due to any surface irregularities.

4. Algorithm of Weighted Least-Squares Fit for Experimental Data

We used a least-squares curve-fitting algorithm to fit the experimental data to provide an empirical relationship between normal forces and areas of contact. A systematic algorithm is developed and presented for doing the least-

squares best fit with a well-defined weighting matrix for various kinds of power equations.[18,19] Taking the logarithmic form of Eq. (18),

$$Ln\ a_{cy} = Ln\ c_{cy} + \gamma_{cy} Ln\ N \qquad (21)$$

with a total of i data sets of (a_{cy}, N) from experiments, Eq. (21) can be rearranged in the following matrix form for least-squares fit:

$$y = A\,x, \qquad (22)$$

where

$$y = \begin{bmatrix} Ln\ a_{cy1} \\ Ln\ a_{cy2} \\ \vdots \\ Ln\ a_{cyi} \end{bmatrix}, A = \begin{bmatrix} 1 & Ln\ N_1 \\ 1 & Ln\ N_2 \\ \vdots & \vdots \\ 1 & Ln\ N_i \end{bmatrix}, x = \begin{bmatrix} Ln\ c_{cy} \\ \gamma_{cy} \end{bmatrix}. \qquad (23)$$

The least-squares solution of x in Eq. (22) can be obtained using the Penrose–Moore generalized inverse that minimizes the norm of errors in y, that is

$$x = A^* y, \qquad (24)$$

where superscript $*$ denotes the generalized inverse. The left inverse is used in Eq. (23), i.e.

$$A^* = (A^T\ \ A)^{-1} A^T. \qquad (25)$$

Table II. The experimental result for exponent γ and constant c by using the weighted least-squares best fit for hemicylindrical and hemispherical soft finger tips.

Type of silicone materials	Hemicylindrical fingertips		Hemispherical fingertips	
	c_{cy}	γ_{cy}	c_{sph}	γ_{sph}
RTV 23	2.8779	0.2427	3.4036	0.2008
RTV 1701	2.2001	0.2712	2.8192	0.2212
RTV 240	1.4944	0.3147	2.2909	0.2441

Equation (24) minimizes the norm of squared errors in $y = \ln N$ instead of N. In order to compensate for such discrepancy, weighted least-squares fit is utilized in the following form:

$$A^* = (W \quad A)^* \, W \, y, \tag{26}$$

where the weighting matrix is $W = \text{diag}[e^{y_1} \ldots e^{y_2}]$ that compensates for the logarithmic scale of the norm of squared errors to be minimized.

5. Results and Discussions

After conducting all the experiments on hemicylindrical and hemispherical fingertips, and applying the weighted least-squares curve fitting, constants of the power law equation, namely γ and c for both fingertip shapes, are obtained as listed in Table II. It can be seen that values of γ for both cases are within the range adopted in the theory, that is $0 \le \gamma_{cy} \le \frac{1}{2}$ and $0 \le \gamma_{sph} \le \frac{1}{3}$.

Figure 5 shows the half contact width, a_{cy}, as a function of the applied normal force, N. The curves indicate that the half contact width is an exponential function of the normal force N, whereas Fig. 6 shows the radius of contact, a_{sph}, as a function of the applied normal force N.

The comparison between the hemicylindrical and hemispherical fingertips shown in Figs. 5 and 6 indicates that when loading both shapes with identical loads, the half width contact of the hemicylindrical fingertip is less than the radius of contact of the hemispherical fingertip. This area of contact can be controlled easily in the case of hemicylindrical fingertip by altering the length of the hemicylinder only, whereas this is limited in the case of hemispherical tip due to axis symmetry. In addition, it was found that hemicylindrical shape fingertips are preferable as compared to spherical shape fingertips, since the width can be maintained constant, while the radius of curvature can be varied, thus yielding the same contact properties as compared with those obtained for larger size spherical fingertips. Furthermore, because silicone of type RTV 240 is a harder material than other types of silicone (RTV 1701 and RTV 23), the observations from the least-squares-fit curve lead us to the conclusion that harder materials tend to have higher exponent values. Normalization of empirical curves can eliminate constant c_{cy} from Eq. (18). The experimental results for the human thumb and index finger[20] show that the human fingers behave like a nonlinear elastic material[21] with γ_{cy} ranging from 0.11 to 0.17. Data taken from Schallamach's work,[22] which are illustrated in Fig. 7, also support our theory. Experimental data for other materials fall within $0 \le \gamma_{cy} \le 1/2$. This is consistent with the theoretical model that the exponent γ_{cy} is within the upper bound $\gamma_{cy} = 1/2$ (for linear elastic materials) and the lower bound $\gamma_{cy} = 0$ (which corresponds to the case of the ideal soft finger). The results of the normalized curves for various materials are plotted in Fig. 7, and are described by the following equation:

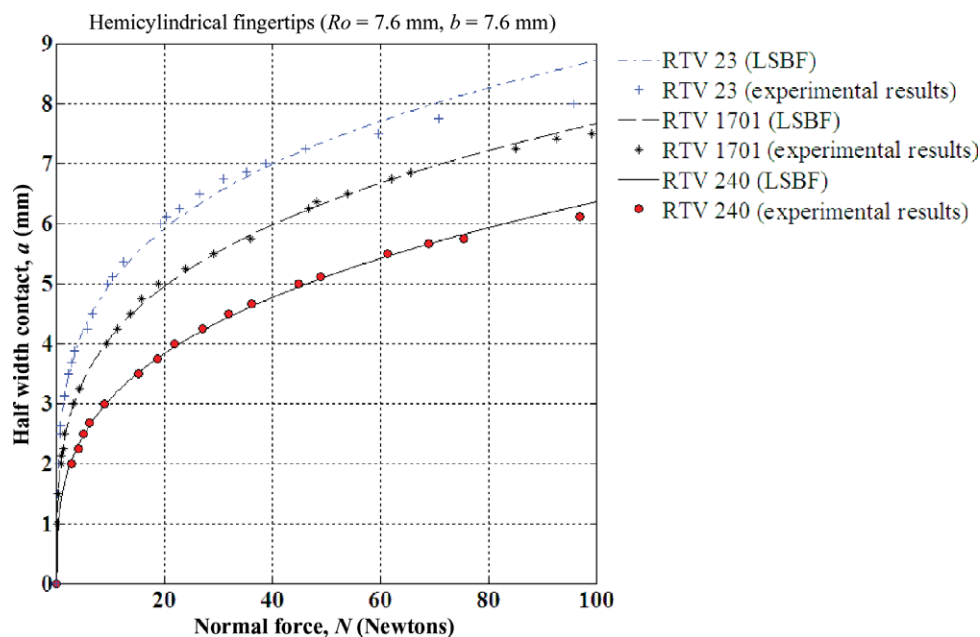$$\left(\frac{a_{cy}}{c_{cy}} \right) = N^{\gamma_{cy}}. \tag{27}$$

Fig. 5. (Colour online) Results of experiments using silicone RTV 23, RTV 1701, and RTV 240 for hemicylindrical fingers ($R_o = 7.6$ mm, $b = 7.6$ mm).
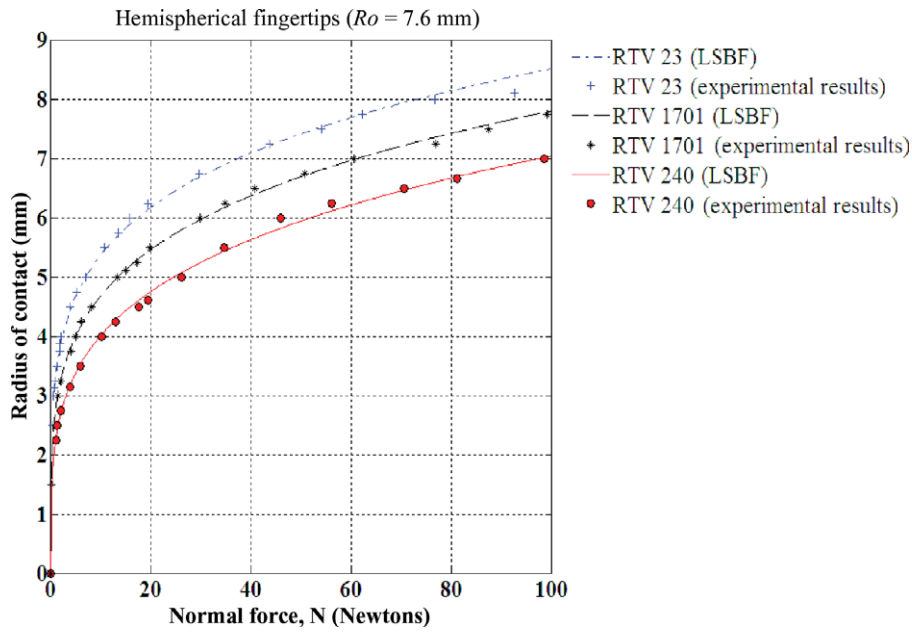
Fig. 6. (Colour online) Results of experiments using silicone RTV 23, RTV 1701, and RTV 240 for hemispherical fingers ($R_o = 7.6$ mm).

The upper and lower bounds of the normalized contact of the half width with respect to the normal force are shown. The experimental results match well with the theoretical derivation of the power law proposed in Eq. (26).

In this study, we showed that the contact model in Eq. (18) could be used for linear elastic contact as well as soft (nonlinear elastic) contact. If the contact is harder and behaves more like linear elastic materials, the exponent in Eq. (19) will be closer to 1/2, reflecting the linear elastic model predicted by Timoshenko and Goodier.[3] Furthermore, since the exponent is between 0 and 1/2, when this exponent becomes larger (e.g. 1/2), the growth rate of the half width is initially smaller but becomes larger than that of the softer contacts with smaller γ_{cy}. On the contrary, a softer finger initially has a rapid half width growth with a subsequently reduced growth rate. This is consistent with the anthropomorphic soft-finger model that we have proposed. If two fingers having exponents of 1 and 2 are considered, we can derive the rate of change of the normalized contact of half width contact with respect to the normal force as

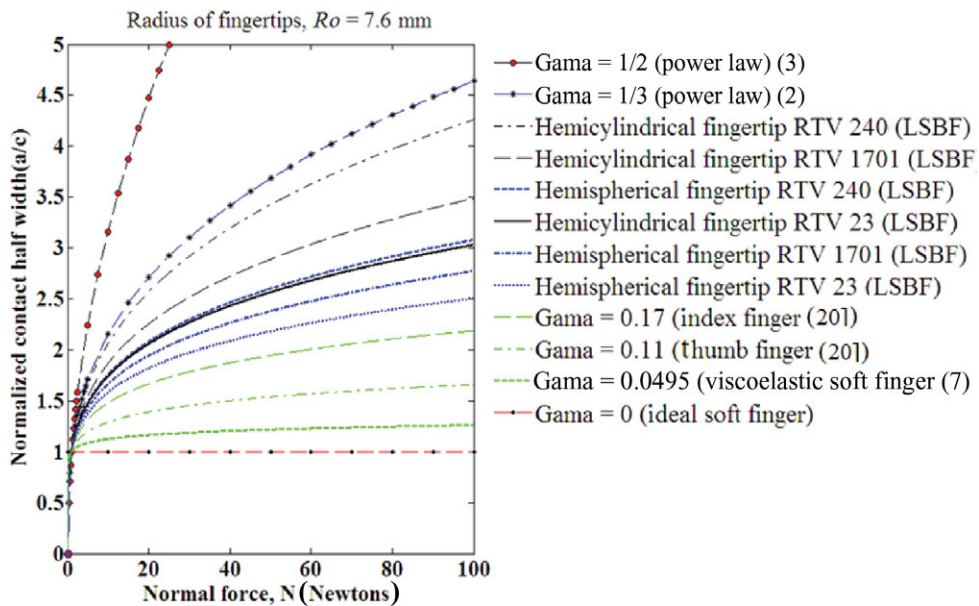$$\frac{d(a_{cy}/c_{cy})}{dN} = \gamma_{cy} N^{(\gamma_{cy}-1)}. \qquad (28)$$

Fig. 7. (Colour online) The normalized half width contact as a function of the normal force $(\frac{a_{cy}}{c_{cy}}) = N^{\gamma_{cy}}$.
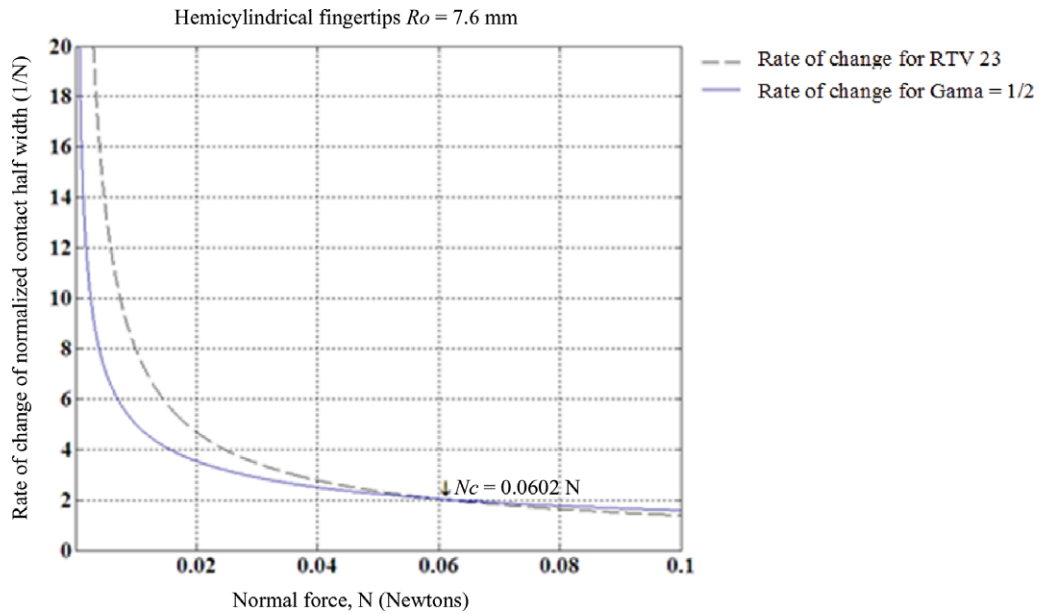
Fig. 8. (Colour online) Comparison of different exponents in the power-law equation for hard finger ($\gamma = \frac{1}{2}$) and soft silicone RTV 23 ($\gamma = 0.2427$) finger.

The rate of change is initially greater for the softer finger. The intersection of the two rates can be found at

$$N_C = e^{-\left(\frac{Ln\gamma_{cy_1} - Ln\gamma_{cy_2}}{\gamma_{cy_1} - \gamma_{cy_2}}\right)}. \tag{29}$$

Equation (29) gives the critical normal force value N_C, at which the rate of change of the contact of the half width is swapped between the two fingers of different exponents.

Figure 7 offers a comparison between two contacts with different values of exponents at each finger harder materials (the linear elastic model) $\gamma_{cy_1} = 1/2$ and softer materials (viscoelastic soft finger) $\gamma_{cy_2} = 0.0495$. We found from Eq.

(29) that $N_C = 0.0059$ N. This intersection is shown in Fig. 7. When the normal force is applied, the initial rate of change in a_{cy} is large, and then it is decreased asymptotically. Below this intersection (i.e. $N < N_C$), the rate of growth of the contact of half width for the softer finger ($\gamma_{cy_2} = 1/10$) is larger than the linear elastic finger ($\gamma_{cy_1} = 1/2$). Above this intersection (i.e. $N > N_C$), the rate of growth of the contact of half width for the softer finger is smaller than that of the linear elastic finger. As the soft finger becomes ideally soft, the initial growth rate of the half width of contact is infinite and then immediately reduces to zero, much like an impulse function. For typical fingers, the critical point N_C is small. As a result, the region of $N < N_C$ occurs very quickly
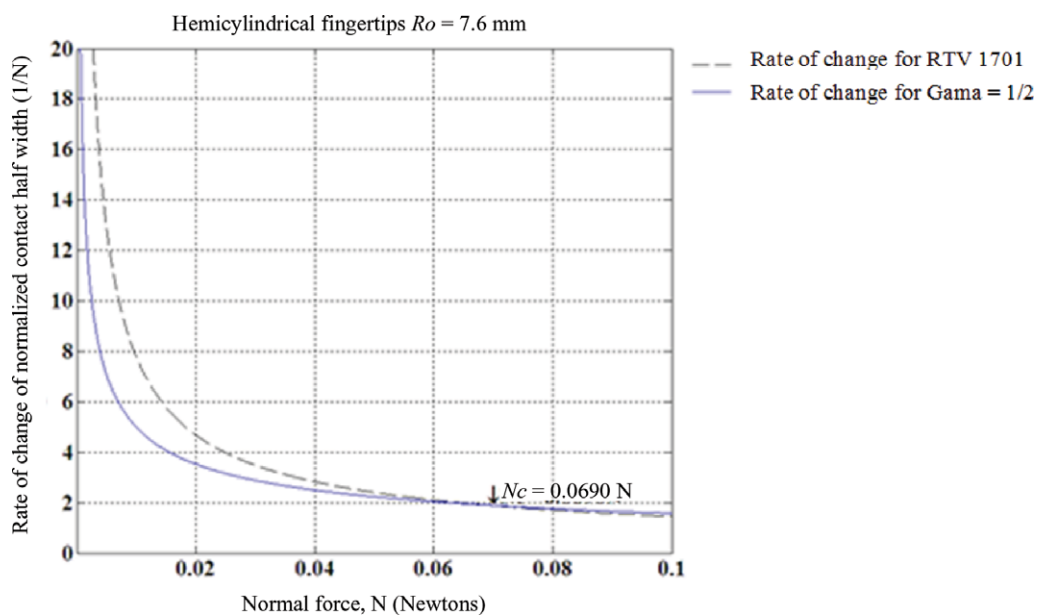

Fig. 9. (Colour online) Comparison of different exponents in the power-law equation for hard finger ($\gamma = \frac{1}{2}$) and soft silicone RTV ($\gamma = 0.2712$) finger.
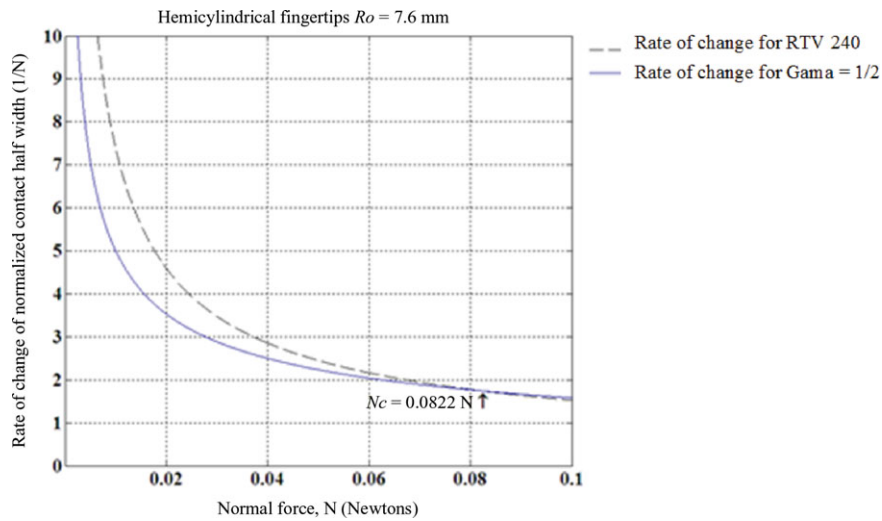
Fig. 10. (Colour online) Comparison of different exponents in the power-law equation for hard finger ($\gamma = \frac{1}{2}$) and soft silicone RTV ($\gamma = 0.3147$) finger.
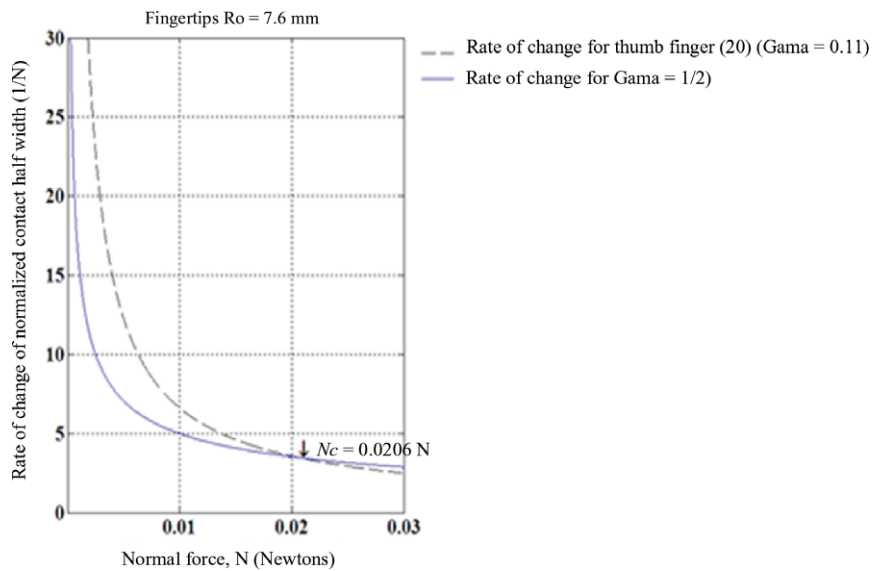
Fig. 11. (Colour online) Comparison of different exponents in the power-law equation for hard finger ($\gamma = \frac{1}{2}$) and thumb finger ($\gamma = 0.11$).
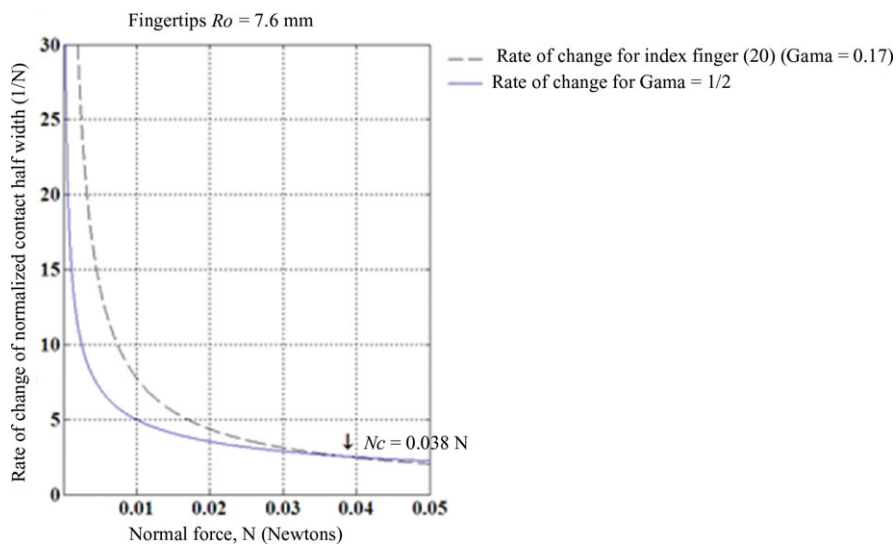
Fig. 12. (Colour online) Comparison of different exponents in the power-law equation for hard finger ($\gamma = \frac{1}{2}$) and index finger ($\gamma = 0.17$).
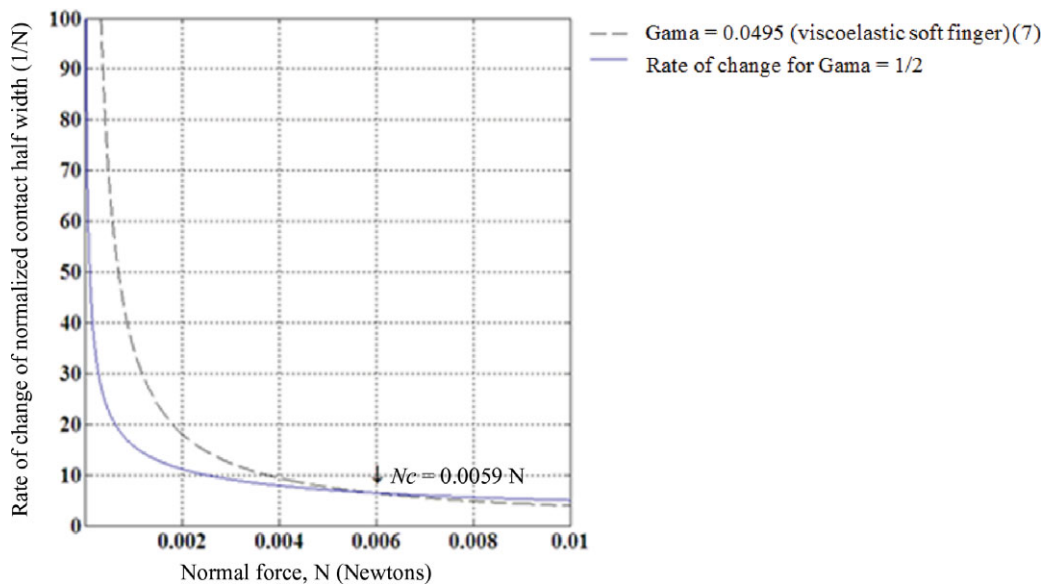
Fig. 13. (Colour online) Comparison of different exponents in the power-law equation for hard finger ($\gamma = \frac{1}{2}$) and viscoelastic finger ($\gamma = 0.0495$).

upon the application of normal force. Figs. 8 to 13 show the rate of change of the normalized half width contact with respect to normal force for different types of hemicylindrical fingertips.

6. Conclusions

A proposed contact-mechanics model for anthropomorphic hemicylindrical soft fingers is proposed as a power-law equation. That is, the half width of contact of a soft finger is proportional to the normal force raised to the power of γ_{cy}, which ranges from 0 to 1/2.

The general result, subsuming the Timoshenko and Goodier[3] contact theory, is in the form of a power equation. The weighted least-squares fit is applied to analyze the experimental data using the theory developed in this work. It is found that the experimental results also match with the range of the theoretical prediction.

It was found that hemicylindrical shape fingertips are preferable over spherical shape fingertips for prosthetic application, since the width can be maintained constant, while the radius of curvature can be varied, thus yielding the same contact properties as compared with those obtained for larger size spherical fingertips.

References

1. M. T. Mason and J. K. Salisbury, *Robot Hands and the Mechanics of Manipulation* (MIT Press, Cambridge, MA, 1985).
2. H. Hertz, "On the Contact of Rigid Elastic Solids and on Hardness," Chapter 6, **In**: *Assorted Papers* (New York, Macmillan, 1882) [Quoted in K. L. Johnson, *Contact Mechanics* (Cambridge University Press, Cambridge, UK, 1985)].
3. S. P. Timoshenko and J. N. Goodier, *Theory of Elasticity*, 3rd ed. (McGraw-Hill, New York, 1970) pp. 414–420.
4. A. Schallamach, "The load dependence of rubber friction," *Proc. Physical Soc.* **65**(9), 657–661 (1969).
5. M. R. Cutkosky, J. M. Jordain and P. K. Wright, "Skin Materials for Robotic Fingers," **In**: *Proceedings of the 1987 IEEE International Conference on Robot and Automat*, Los Alamitos, CA (1987) pp. 1649–1654.
6. H.-Y. Han, A. Shimada and S. Kawamura "Analysis of Friction on Human Fingers and Design of Artificial Finger," **In**: *Proceedings of the 1996 IEEE International Conference on Robot and Automat*, Washington, DC (1996), pp. 3061–3066.
7. N. Xydas and I. Kao, "Modeling of Contact Mechanics with Experimental Results for Soft Fingers," **In**: *Proceedings of the 1998 IEEE/RSJ International Conference on Intelligent Robots and Systems*, Victoria, BC, Canada (Oct. 1998) pp. 488–493.
8. N. Xydas and I. Kao, "Modeling of contact mechanics and friction limit surface for soft fingers with experimental results," *Int. J. Robot, Res.* **18**(9), 941–950 (Sep. 1999).
9. I. Kao and F. Yang, "Stiffness and contact mechanics for soft fingers in grasping and manipulation," *IEEE Trans. Robot. Autom.* **20**(1) (Feb. 2004) pp. 132–135.
10. K.-H. Park, B.-H. Kim and S. Hirai, "Development of a Soft-Fingertip and Its Modeling Based on Force Distribution," **In**: *Proceedings of the 2003 IEEE.International Conference on Robotics & Automation*, Taipei, Taiwan (Sep. 14–19, 2003) pp. 14–19.
11. T. Inoue and S. Hirai, "Elastic model of deformable fingertip for soft-fingered manipulation," *IEEE Trans. Robot.* **22**(6), 1273–1279 (Dec. 2006).
12. K. Hosoda, Y. Tadaa and M. Asada, "Anthropomorphic robotic soft fingertip with randomly distributed receptors," *Robot. Auton. Syst.* **54**, 104–109 (2006).
13. F. Ficuciello, "Modelling and Control for Soft Finger Manipulation and Human-Robot Interaction," *Ph.D. Thesis* (Faculty of Engineering, University of Naples Federico II, Italy, 2010).
14. V. A. Ho and S. Hirai, "Understanding Slip Perception of Soft Fingertips by Modeling and Simulating Stick-Slip Phenomenon," **In**: *Proceedings of the Robotics: Science and*

Systems VII Conference, University of Southern California, LA, USA (2011), available at: http://robotics.usc.edu/rss2011/.

15. J. W. Hutchinson, "Fundamentals of the phenomenological theory of nonlinear fracture mechanics," *Trans. ASME, J. Appl. Mech.* **50**, 1042–1051 (1983).
16. Suter-Kunststoffeag, *Manual of Swiss-Composite Group.* www.swiss-compsite.ch 2009.
17. *Manual of Zwick Tensile Tester*, EGR 281 (winter 2007), available at: http://www.zwick.co.uk/en.html.
18. W. Y. Yang, W. Cao, T. S. Chung and J. Morris, *Applied Numerical Methods Using Matlab* (John Wiley, Hoboken, NJ, 2005).
19. Q. Lin, J. W. Burdick and E. Rimon, "A stiffness-based quality measure for compliant grasps and fixtures," *IEEE Trans. Robot. Automat.* **16**, 675–688 (Dec. 2000).
20. H. Kinoshita, L. Backstrom, J. R. Flanagan and R. Johansson "Tangential torque effects on the control of grip forces when holding objects with precision grip," *J. Neurophys.* **78**(3), 1619–1630 (1997).
21. Y. C. Fung *Biomechanics, Medical Properties of Living Tissues*, 2nd ed. (Springer-Verlag, New York, 1993).
22. A. Schallamach, "The load dependence of rubber friction," *Proc. Physical Soc.* **65**(9), 657–661 (1969).